

AugLift: Boosting Generalization in Lifting-based 3D Human Pose Estimation

Nikolai Warner¹, Wenjin Zhang², Irfan Essa¹, Apaar Sadhwani^{3*}

¹Georgia Institute of Technology

²Rutgers University

³Stanford University

nwarner30@gatech.edu, wz315@scarletmail.rutgers.edu, irfan@cc.gatech.edu, apaars@stanford.edu

Abstract

Lifting-based methods for 3D Human Pose Estimation (HPE), which predict 3D poses from detected 2D keypoints, often generalize poorly to new datasets and real-world settings. To address this, we propose *AugLift*, a simple yet effective reformulation of the standard lifting pipeline that significantly improves generalization performance without requiring additional data collection or sensors. AugLift sparsely enriches the standard input—the 2D keypoint coordinates (x, y) —by augmenting it with a keypoint detection confidence score c and a corresponding depth estimate d . These additional signals are computed from the image using off-the-shelf, pre-trained models (e.g., for monocular depth estimation), thereby inheriting their strong generalization capabilities. Importantly, AugLift serves as a modular add-on and can be readily integrated into existing lifting architectures.

Our extensive experiments across four datasets demonstrate that AugLift boosts cross-dataset performance on unseen datasets by an average of 10.1%, while also improving in-distribution performance by 4.0%. These gains are consistent across various lifting architectures, highlighting the robustness of our method. Our analysis suggests that these sparse, keypoint-aligned cues provide robust frame-level context, offering a practical way to significantly improve the generalization of any lifting-based pose estimation model. Code will be made publicly available.

1 Introduction

Monocular 3D Human Pose Estimation (HPE) seeks to reconstruct 3D skeletal structures from 2D images or videos. A dominant and effective paradigm for this task is the *lifting-based* approach, where 2D keypoints are first detected in an image and then “lifted” to 3D space via a learned model (Martinez et al. 2017; Pavllo et al. 2018; Zhu et al. 2023). While this problem decomposition reduces complexity, the lifting process is inherently ill-posed: a single 2D pose can correspond to multiple valid 3D poses, a problem exacerbated by occlusions. To resolve this ambiguity, some methods leverage temporal context from video sequences (Pavllo et al. 2018; Zhu et al. 2023), while others attempt to condition the lifting model on image features (Xu et al. 2022; Zhou, Yin, and Li 2024). However, these image-based approaches often struggle to generalize, with learned

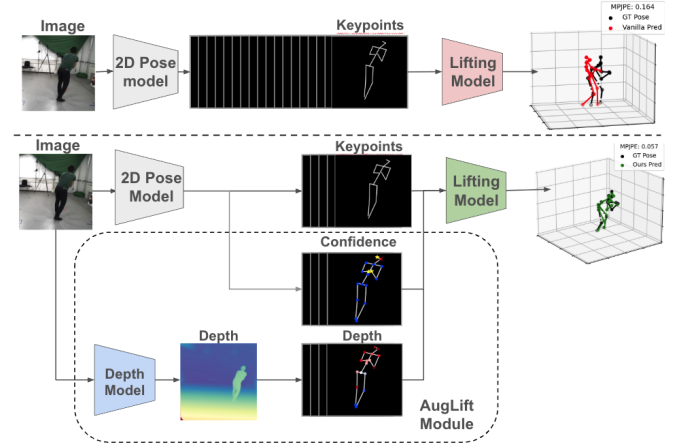


Figure 1: **AugLift Enriches Standard Lifting Inputs for Better Generalization.** A standard lifting model (*top*) relies on sparse 2D coordinates (x, y) , leading to ambiguity. *AugLift* (*bottom*) reformulates the input as a 4D vector (x, y, c, d) by appending a detector confidence score c and a depth estimate d . Sourced from off-the-shelf models, these cues provide crucial context on keypoint reliability and location, improving generalization without requiring architectural changes or additional data collection.

priors sometimes focusing more on background pixels than the subject itself (Zhou, Yin, and Li 2024).

Despite these advances, a critical challenge remains: modern 3D HPE models exhibit poor generalization when moving from controlled lab datasets to real-world settings. Recent benchmarks show that state-of-the-art lifting networks achieving 40–50mm MPJPE on the Human3.6M dataset can degrade to over 100mm on in-the-wild datasets like 3DPW when using detected 2D keypoints (Manzur et al. 2025; Wang, Shin, and Fowlkes 2020). We identify two primary factors contributing to this degradation. First, there is a key disconnect in how lifting pipelines are developed versus how they are applied. Architectures are typically benchmarked on clean, ground-truth 2D keypoints, but must operate on noisy detections in the wild. Simply fine-tuning on these detections represents a missed opportunity, as it discards valuable contextual information from the 2D detector—such as

*Corresponding author.

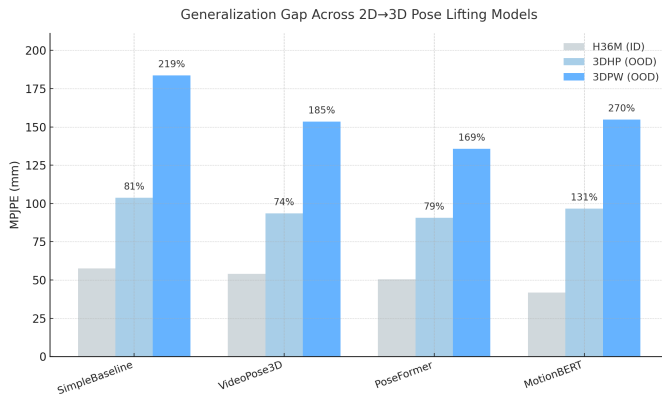


Figure 2: **Modern lifting models generalize poorly across datasets.** We plot the in-distribution (ID) MPJPE on H3.6M against out-of-distribution (OOD) performance on 3DHP and 3DPW for four popular architectures. Percentages show the OOD error inflation, with even state-of-the-art models exhibiting gaps of over 150%. See Table 2 and Section 4.3 for detailed results.

keypoint confidence scores—that could help resolve ambiguity. Second, a significant domain gap exists between training datasets and real-world environments. Most large-scale 3D pose datasets are captured in controlled laboratory settings, which cannot account for the sheer diversity of camera angles, subject appearances, actions, and backgrounds encountered in unconstrained scenarios. While creating new, more diverse 3D datasets could address the second factor, it remains prohibitively expensive and does not solve the first. Our goal is therefore to improve the generalization of lifting-based models by addressing both factors *without* requiring additional data collection or specialized hardware.

To this end, we introduce *AugLift*, a simple and effective reformulation of the standard lifting pipeline. AugLift enriches the input to a lifting model by augmenting the standard 2D keypoint coordinates (x, y) with two additional signals: a detection confidence score c and a corresponding depth estimate d . These cues are obtained directly from the input image using off-the-shelf, pre-trained models, allowing AugLift to inherit their robust generalization capabilities at no extra data-collection cost. By design, AugLift functions as a lightweight, add-on module that can be readily integrated into any existing lifting architecture, typically by only modifying the input layer. Other minor but helpful components of AugLift, such as bounding-box rescaling to account for camera-distance shifts, are detailed in the Methods section.

We validate our approach through a series of comprehensive experiments. We demonstrate that across four diverse datasets and four different lifting architectures, AugLift consistently and significantly improves performance in both cross-dataset (out-of-distribution) and within-dataset (in-distribution) scenarios. For instance, when integrated with a state-of-the-art model (MotionBERT (Zhu et al. 2023)), AugLift boosts cross-dataset performance by an average of

10.1% while simultaneously improving in-distribution performance by 4.0%, as measured by the reduction in MPJPE.

Our key contributions are as follows:

- We propose *AugLift*, a novel reformulation of the standard lifting-based 3D HPE. It is a simple, add-on module to any existing architecture that augments 2D keypoint coordinates with confidence scores and depth estimates using off-the-shelf models, requiring no new data or sensors at training or inference.
- We demonstrate **significant generalization gains**, showing through extensive cross-dataset experiments that AugLift consistently improves the performance of lifting models on unseen data by an average of 10.1%.
- We establish the **robustness and broad applicability** of our approach by showing that AugLift delivers performance improvements across multiple distinct lifting architectures, confirming it as a general-purpose enhancement for the field.

2 Literature Review

Research in monocular 3D human pose estimation has progressed along several distinct avenues. In the following, we provide a structured review of the relevant literature along these themes—2D-to-3D lifting, generalization strategies, and weakly supervised learning—before discussing methods that enrich the lifting input, which is most relevant to our work.

2D-to-3D Lifting. The paradigm of lifting 2D keypoints to 3D space gained prominence after Martinez et al. (Martinez et al. 2017) demonstrated that a simple, fully-connected network could achieve competitive results by operating directly on 2D coordinates. This approach, however, struggles with the inherent ambiguity of single-frame inputs. To mitigate this, temporal models were introduced. For instance, VideoPose3D (Pavlo et al. 2018) leverages temporal convolutions over sequences of 2D poses to enforce motion consistency. More recently, Transformer-based architectures like MotionBERT (Zhu et al. 2023) have become state-of-the-art by jointly modeling spatial and temporal relationships in human motion. Despite their success, these foundational methods still face challenges with occlusions and depth ambiguities, motivating the need for richer input signals.

Generalization Strategies. Improving generalization to unseen datasets and real-world scenarios remains a primary challenge. Several strategies focus on data augmentation and architectural enhancements. PoseAug (Gong, Zhang, and Feng 2021), for example, uses virtual camera augmentations to simulate multiple perspectives during training, thereby improving robustness. Other works propose multitask learning; Wang et al. (Wang, Shin, and Fowlkes 2020) integrate 3D pose estimation with camera viewpoint prediction to leverage complementary information. Rhodin et al. (Rhodin, Salzmann, and Fua 2018) use a geometry-aware encoder-decoder framework to learn from multi-view images in a semi-supervised fashion. While effective, these methods often introduce significant architectural complexity or require specialized training data.

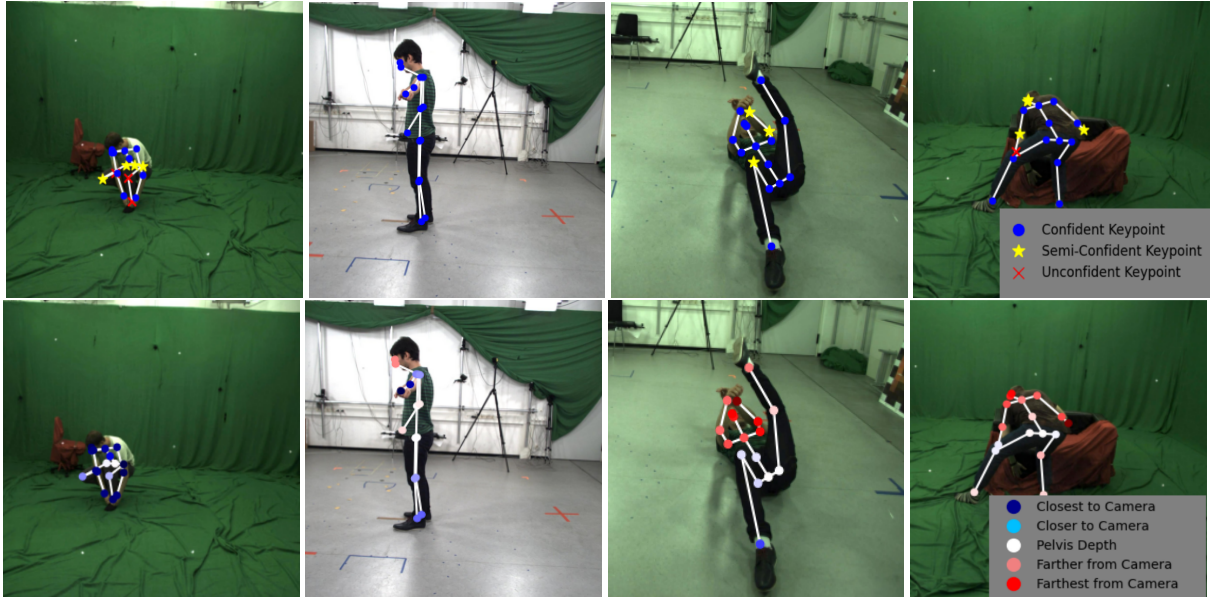


Figure 3: **The Synergistic Input Cues of AugLift.** We visualize the confidence (*top*) and depth (*bottom*) signals that augment the standard lifting input. Confidence scores act as a proxy for visibility (blue = confident, red X = unconfident), while the depth map (blue = near, red = far) captures the 3D structure. The synergy is key: confidence scores help the model identify and distrust unreliable depth estimates that often occur at occluded joints, leading to a more robust lifting process.

Weakly-Supervised and Unsupervised Learning. Given the high cost of acquiring 3D annotations, methods that reduce reliance on labeled data are crucial. Unsupervised approaches, such as the one by Chen et al. (Chen et al. 2019), enforce geometric self-consistency through a lift-reproject-lift cycle, using a 2D pose discriminator to ensure plausible skeletons without any 3D priors. Semi-supervised techniques, explored by Pavlo et al. (Pavlo et al. 2018), combine limited 3D ground truth with a larger corpus of 2D data by minimizing a reprojection loss. These methods showcase how geometric constraints can substitute for explicit 3D labels.

Enriching Lifting with Image-Derived Cues. To overcome the limitations of using only 2D coordinates, another key line of research has explored enriching the input with cues derived directly from the source image. One approach involves creating hybrid models that condition the lifter on rich visual features from a CNN backbone (Nie et al. 2019; Xu et al. 2022). However, this strategy faces a critical generalization challenge, as these dense features often learn spurious correlations with the training set’s background and appearance (Zhou, Yin, and Li 2024). To avoid these pitfalls, other works utilize more targeted, semantic signals. For instance, the confidence scores from a 2D detector have been used in isolation to improve robustness to noisy detections (Gong, Zhang, and Feng 2021). Separately, other methods incorporate depth-related information—most commonly as relative ordinal rankings (Pavlakos, Zhou, and Daniilidis 2018; Jiang 2021)—to address depth ambiguity. A key limitation of these specialized approaches, however, is that they require the true depth information for model training, creating a data bottleneck. In contrast, AugLift bypasses this data

bottleneck by harnessing pretrained models with strong generalization. Further, as we shall see the true potential lies not in using isolated cues, but in the joint use of confidence and depth estimate, which is superior to prior art. Examples of our complementary inputs are shown in Figure 3.

3 Methods

3.1 Motivation and Insights

The design of AugLift was guided by preliminary analyses aimed at understanding the failure modes of modern lifting-based methods. We summarize our key findings and the resulting design principles below.

Motion Cues Can Harm Generalization. A common assumption in 3D HPE is that temporal information should improve performance. Our investigation challenges this assumption in the context of cross-dataset generalization. To isolate the effect of motion dynamics from detection noise, this specific analysis was performed using ground-truth 2D keypoints. While longer motion sequences consistently reduce in-distribution error, we found they typically degrade performance on out-of-distribution datasets (see Appendix, Fig. 5). To probe this further, we tested models on unseen motion patterns composed of familiar poses (e.g., reversed or sped-up sequences) and observed a significant performance drop. This indicates that temporal models overfit to the limited motion dynamics present in the training data. We conjecture this occurs because the combinatorial space of valid human motions is vastly larger than the space of static poses, making it difficult to generalize from the motion examples in current datasets. This suggests that instead of over-relying on brittle motion priors, a more robust path

Algorithm 1: The AugLift Module.

Input: Image I containing the human subject.

Step 1: Obtain 2D Keypoints with Confidence Scores

This step is unchanged from standard lifting. We run inference on image I using a 2D keypoint detector to obtain the keypoints with confidence, $\{(x_j, y_j, c_j)\}_{j=1}^K$.

Step 2: Construct Keypoint Depth Estimates

- i. Run inference with a Depth Estimation model on image I to obtain depth map D .
- ii. Compute robust depth estimate $d_j = \min_{(u,v) \in \mathcal{N}_j} D(u, v)$ using a local neighborhood $\mathcal{N}_j = \{(u, v) : \|(u, v) - (x_j, y_j)\|_2 \leq r\}$ for each keypoint $j = 1, \dots, K$.

Step 3: Rescale 2D Keypoints per Normalized Bounding Box

- i. Compute keypoint centroid: $c = (\frac{1}{K} \sum_j x_j, \frac{1}{K} \sum_j y_j)$.
- ii. Compute box size (average of width and height):
 $b = \frac{1}{2} [(\max_j x_j - \min_j x_j) + (\max_j y_j - \min_j y_j)]$.
- iii. Compute scale factor $s = \bar{b}/b$, where \bar{b} is the mean training-set box size.
- iv. Update $(x_j, y_j) := s \cdot ((x_j, y_j) - c) + c$ for all j .

Step 4: Normalize Confidence and Depth

- i. Rescale confidence to $[-1, 1]$: $\tilde{c}_j = 2c_j - 1$ for all j .
- ii. Obtain root-relative depths: $\tilde{d}_j = d_j - d_{\text{root}}$ for all j .
- iii. Clip root-relative depths so $\tilde{d}_j \in [0, \tilde{d}_{\text{max}}]$ for all j .

Output: 4D feature vector $\tilde{q}_j = (x_j, y_j, \tilde{c}_j, \tilde{d}_j)$ for keypoints $j = 1, \dots, K$. These augmented features serve as inputs for lifting.

to generalization lies in strengthening the input signal for each individual frame.

Per-Frame Depth Cues Offer a Robust Alternative.

Given the fragility of motion cues, we investigated the potential of enriching the per-frame input instead. As discussed in the Literature Review, a number of prior works have explored this direction using various image-derived cues. Our own analysis focused on the impact of *depth cues* as a particularly promising signal. To establish an upper bound on their potential, we conducted oracle experiments using privileged, ground-truth ordinal depth information at varying granularities. The results were compelling: augmenting the sparse (x, y) input with even coarse, three-bin ordinal depth information, for instance, cut the cross-dataset error (H3.6M→3DPW) by approximately 25% (see Appendix, Table 11). This demonstrated that providing the lifter with even basic geometric context is a powerful and robust path toward better generalization, forming the primary motivation for our work.

Design Principles. Guided by our analyses, we established three core principles for AugLift. Our approach must: (1) harness richer frame-level inputs to improve generalization; (2) be a modular add-on that preserves the simplicity of lifting architectures; and (3) avoid new data collection by instead harnessing the strong generalizable priors from off-the-shelf pretrained models.

3.2 The AugLift Method

The AugLift method is a lightweight pre-processing pipeline designed to be a modular add-on to any existing lifting-

based model. It transforms the standard 2D keypoint inputs into a richer 4D representation to improve generalization, without altering the core lifting architecture. The full procedure is detailed in Algorithm 1.

The core of AugLift is the augmentation of each 2D keypoint (x_j, y_j) with two additional signals: a detector confidence score c_j and a metric depth estimate d_j . The confidence score, provided directly by the 2D detector, serves as a powerful proxy for joint visibility and reliability. The depth estimate is sourced from an off-the-shelf monocular depth estimation model. To ensure robustness against noise and occlusions, we don’t just sample the depth at the keypoint’s exact location; instead, as shown in Step 2 of Algorithm 1, we take the minimum depth value in a small local neighborhood. This captures the depth of the nearest occluding surface, providing a more reliable geometric cue. It is crucial to interpret this signal correctly: for an occluded keypoint, this value serves as a robust lower bound on its true depth, while for a visible keypoint, it provides a precise metric estimate—a much richer signal than the relative ordinal rankings used in prior work.

Before being passed to the lifting model, the inputs undergo two normalization procedures that help improve generalization. First, to handle variations in camera distance from those seen at training, we standardize the skeleton’s scale by applying a bounding box rescaling transformation to the (x, y) coordinates (Step 3). Second, the new feature channels are normalized (Step 4): confidence is mapped to $[-1, 1]$, and the depth values are made root-relative and clipped to a maximum value, d_{max} . This helps, for example, assign a reasonable no-information default when dropout zeroes out the confidence signal at training. In our experiments, we use a neighborhood radius of $r = 3$ pixels for depth sampling and a maximum relative depth of $d_{\text{max}} = 2$ meters.

Integrating this final 4D input vector requires only a minimal change to the lifting model: the input layer’s width is simply expanded to accept $4K$ channels instead of the original $2K$, leaving all deeper layers untouched.

With the AugLift pre-processing in place, the modified lifting model is then trained using the original training data. All training and inference are performed in the detection setting (i.e., using detected, not ground-truth, 2D keypoints). This is essential for two reasons: it minimizes the domain gap to real-world scenarios, and it is a prerequisite for our method, as the confidence score c_j is only defined for detected keypoints.

4 Experiments

4.1 Experimental Setup

Datasets. We conduct experiments on four diverse 3D HPE datasets: Human3.6M (H36M) (Ionescu et al. 2014), MPI-INF-3DHP (3DHP) (Mehta et al. 2016), Fit3D (Fieraru et al. 2021), and 3D-Pose-in-the-Wild (3DPW) (von Marcard et al. 2018). Each dataset offers unique challenges: H36M consists of controlled indoor motions, 3DHP has greater viewpoint diversity, Fit3D contains varied fitness motions, and 3DPW is a challenging in-the-wild dataset

Table 1: **AugLift improves both cross-dataset (OOD) and in-distribution (ID) performance, regardless of the training dataset.** We show raw MPJPE (mm) for the MotionBERT baseline versus the AugLift-enabled model when trained on three different source datasets. The mean improvement is 10.1% for OOD and 4.0% for ID settings.

Train DS	Variant	H36M	3DHP	Fit3D	3DPW
H36M	Baseline	41.8	96.7	66.6	154.8
	AugLift	40.7	85.9	55.8	146.9
	Δ	2.6%	11.2%	16.2%	5.1%
3DHP	Baseline	80.9	52.2	88.2	130.3
	AugLift	79.3	50.9	76.8	121.3
	Δ	2.0%	2.5%	12.9%	6.9%
Fit3D	Baseline	127.4	166.1	39.9	195.4
	AugLift	109.1	132.9	37.1	191.3
	Δ	14.4%	20.0%	7.0%	2.1%

with complex activities and dense occlusions. To thoroughly evaluate generalization, we use H36M, 3DHP, and Fit3D for both training and testing, leveraging their corresponding splits. Due to its smaller size, 3DPW is used exclusively as a test set. While we train on different datasets, H36M serves as our default training set for experiments where the training data is fixed.

Lifting Architectures. To demonstrate that AugLift is a modular add-on, we integrate it into four representative lifting backbones: the Transformer-based MotionBERT (Zhu et al. 2023) and PoseFormer (Zheng et al. 2021), the TCN-based VideoPose3D (Pavlo et al. 2018), and the MLP-based SimpleBaseline (Martinez et al. 2017). Together, these popular models represent a diverse range of lifting paradigms, from simple MLPs and temporal convolutions to state-of-the-art Transformers. As a recent, state-of-the-art model, MotionBERT serves as our default lifting architecture for cross-dataset experiments.

Evaluation Protocol. Following standard practice, we measure performance using Mean Per Joint Position Error (MPJPE) in millimeters. We report both in-distribution (ID) performance on the validation split of the training dataset and out-of-distribution (OOD) performance on other datasets to assess generalization. Crucially, all main experiments are conducted in the “detection setting,” where models are trained and tested on 2D keypoints produced by a detector, not ground truth. This aligns our evaluation with real-world application. To ensure a fair and unified comparison, we use a single off-the-shelf 2D detector (RTMPose-L (Jiang et al. 2023)) and depth estimation model (Depth Anything v2 (Li et al. 2024)) for all experiments. Accordingly, we train both the original backbones and their AugLift-enabled counterparts on the keypoints produced by this detector. As a result, our baseline MPJPE scores may differ slightly from those reported in prior work, which rely on H36M-tuned detectors or ground-truth keypoints that are incompatible with our protocol.

4.2 Cross-Dataset Study

Does AugLift improve performance on unseen datasets? Does it help—or harm—accuracy on the source dataset itself? We conduct a rigorous study to answer these questions.

We train a baseline lifting model and its AugLift-enabled counterpart in three independent training runs, each on a different source dataset—H36M, 3DHP, and Fit3D. After training, every model is evaluated on all four datasets (H36M, 3DHP, Fit3D, 3DPW), in line with our Evaluation Protocol in Section 4.1. This yields one ID and three OOD scores per run. Using three distinct training distributions ensures our findings are robust and not biased by a single dataset. For this study, we use the state-of-the-art MotionBERT backbone.

The results, summarized in Table 1, show that **AugLift improves accuracy in every ID and OOD scenario**. Averaged across all three training regimes, AugLift improves OOD performance by a mean of **10.1%** and also boosts ID performance by a mean of **4.0%**. The OOD gains are most pronounced under large domain shifts; for example, training on Fit3D and testing on 3DHP yields a 20.0% error reduction. These findings demonstrate that AugLift is a powerful mechanism for improving generalization without sacrificing in-domain accuracy.

4.3 Cross-Architecture Study

Do the gains from AugLift span different lifting architectures? Furthermore, is the combination of both confidence and depth critical to its performance? Having established that AugLift provides robust generalization across datasets, we conduct a deeper study to answer these questions.

We evaluate four distinct and popular lifting backbones: SimpleBaseline, VideoPose3D, PoseFormer, and MotionBERT, as detailed in Section 4.1. For each backbone, we train and evaluate three variants: the standard baseline, a baseline augmented with only confidence scores, and the full AugLift-enabled model. All models in this study are trained on H36M and evaluated on both in-distribution (H36M) and out-of-distribution (3DHP, Fit3D, and 3DPW) test sets.

The results, presented in Table 2, confirm that AugLift consistently improves performance across all four architectures. On average, AugLift reduces OOD error by **8.9%** and ID error by **2.3%**. Notably, the simplest model, SimpleBaseline, receives one of the largest OOD improvements at 11.7%, suggesting that the explicit geometric cues provided by AugLift may be particularly beneficial for models with less capacity to learn such relationships implicitly.

Furthermore, this **experiment highlights the critical synergy between the confidence and depth cues**. As shown in Table 2, augmenting the baseline models with only confidence scores yields negligible or inconsistent gains. The significant and consistent performance boost is only unlocked when both confidence and depth are used jointly: the depth offers a precise signal for visible keypoints and a lower-bound for occluded ones, while the confidence (which strongly correlates with keypoint visibility) helps distinguish between these two cases. It is this fusion of a reliability signal (confidence) with a geometric signal (depth) that pro-

Table 2: **AugLift provides robust gains across diverse architectures, and the synergy of confidence and depth is critical.** Raw MPJPE (mm) on H36M (ID) and three OOD sets. Adding only confidence provides marginal benefits, while the full AugLift model delivers significant ID and OOD improvements across all backbones. The mean improvement for AugLift over the baseline is 2.3% for ID and 8.9% for OOD performance.

Architecture	Variant	In-Distribution		Out-of-Distribution			
		H36M	Δ_{ID} (%)	3DHP	Fit3D	3DPW	Δ_{OOD} (%)
MotionBERT	Base Model	41.8	—	96.7	66.6	154.8	—
	Base Model + confidence	41.3	—	92.6	63.6	151.0	—
	Base Model + AugLift	40.7	2.6%	85.9	55.8	146.9	10.8%
SimpleBaseline	Base Model	57.5	—	103.8	81.6	183.7	—
	Base Model + confidence	58.5	—	101.4	84.0	167.5	—
	Base Model + AugLift	54.6	5.0%	96.1	75.2	147.4	11.7%
VideoPose3D	Base Model	53.9	—	93.6	79.2	153.4	—
	Base Model + confidence	55.0	—	93.5	80.5	146.2	—
	Base Model + AugLift	53.8	0.2%	89.8	75.5	140.8	5.7%
PoseFormer	Base Model	50.5	—	90.6	75.3	135.6	—
	Base Model + confidence	51.3	—	90.6	76.0	129.7	—
	Base Model + AugLift	49.8	1.4%	83.8	70.2	124.5	7.6%

vides the rich, robust input needed for generalized 3D pose estimation.

4.4 Deeper Analysis and Discussion

We conduct two key ablation studies analyzing the impact of our bounding box rescaling and the effect of sequence length on AugLift’s performance. We provide a qualitative analysis to visually inspect the improvements from AugLift, followed by an initial analysis of the inference latency.

Impact of Bounding Box Rescaling. Our bounding box rescaling (Step 3 in Algorithm 1) is designed to normalize for variations in camera distance, a common challenge in OOD settings. Indeed, dataset statistics reveal significant differences in subject depth across benchmarks (Table 3). Subjects in 3DPW, for example, are much closer to the camera (mean depth 3.29m) than in the H36M training set (5.67m), resulting in out-of-distribution bounding box sizes. While prior work like PoseDA (Chai et al. 2023) has addressed this, their approach requires access to test set summary statistics. In contrast, our method performs a per-instance normalization, using the on-the-fly depth estimates to adapt to each test example individually without privileged information. As shown in Table 4, this provides significant gains on the 3DPW dataset where the domain gap is largest, reducing error by up to 14.3%. Crucially, the gains from this rescaling are independent of whether the core AugLift cues are used, suggesting it is a broadly beneficial component in combating train-test domain gaps. We note, however, that it does not benefit all architectures; for instance, MotionBERT already incorporates a camera-invariance mechanism, making our rescaling redundant.

Impact of Sequence Length. We now analyze how AugLift’s benefits vary with the amount of temporal information available to the model. In this study, we use the default settings from Section 4.1 (MotionBERT architecture trained on H36M) and evaluate it across a range of sequence lengths. For each sequence length, we report the in-

Table 3: **Dataset statistics reveal a significant domain gap in subject depth.** The mean depth for 3DPW differs substantially from the primary training set, H36M.

Dataset	Mean Depth	Depth (10%–90%)
H36M	5.67m	4.58–6.53m
3DHP	5.05m	3.74–6.31m
Fit3D	5.00m	4.45–5.28m
3DPW	3.29m	2.20–4.50m

Table 4: **Per-instance bounding box rescaling improves performance on the OOD 3DPW dataset.** We report MPJPE (mm) with and without our on-the-fly rescaling enabled. It is broadly beneficial, even in the absence of other AugLift components.

Architecture	Variant	Rescaling		Δ (%)
		No	Yes	
SimpleBaseline	Baseline	182.5	156.4	14.3%
	AugLift	164.5	147.4	10.0%
VideoPose3D	Baseline	168.3	161.4	4.0%
	AugLift	147.4	140.8	4.5%

distribution (ID) improvement on H36M and the mean out-of-distribution (OOD) improvement averaged over the three other test sets (3DHP, Fit3D, and 3DPW).

The results, summarized in Table ??, reveal a key trend: while the in-distribution gains from AugLift taper as more temporal context is added, the out-of-distribution gains remain substantial. For single-frame models (Seq-Len 1), AugLift reduces OOD error by a significant **11.7%**. Even for very long sequences (Seq-Len 243), where the baseline model is already very strong, AugLift still delivers a robust **8.3%** OOD error reduction. This strongly supports our hypothesis that the rich, per-frame spatial cues provided by

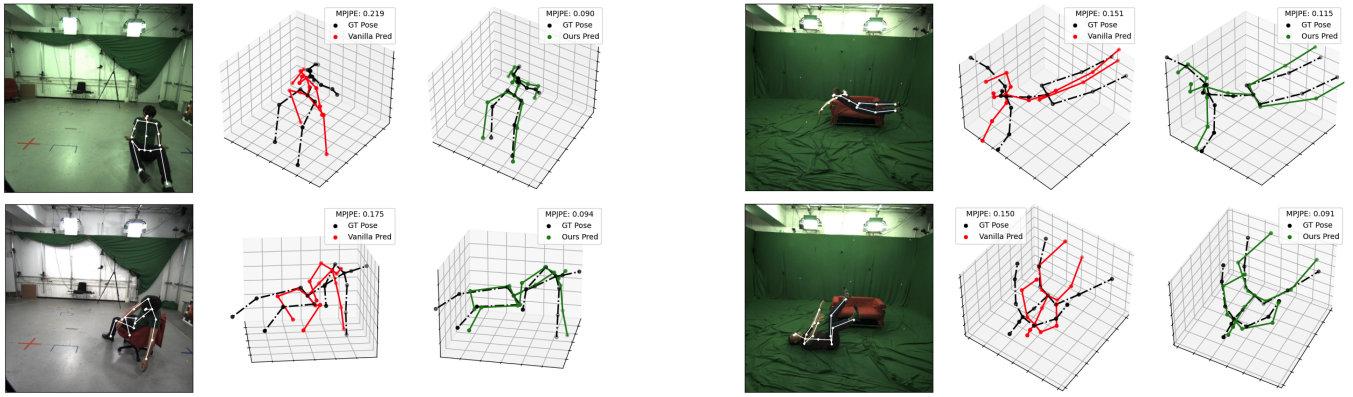


Figure 4: **Qualitative comparison of a baseline model versus the AugLift-enabled model on challenging poses.** In these examples, MotionBert was trained on H36M and tested on the OOD 3DHP dataset. The ground truth pose is shown in black, the baseline prediction in red, and the AugLift prediction in green. AugLift consistently produces more accurate 3D poses, especially for ambiguous scenarios like sitting and crouching where its additional depth and confidence cues are most vital.

Table 5: **AugLift’s OOD benefits are substantial across all sequence lengths.** We show the percentage improvement (%) for MotionBERT trained on H36M. Δ_{AugLift} is the gain of the full model over the baseline. Δ_{Depth} shows the marginal gain from adding the depth cue to a model that already uses confidence.

Seq-Len	Split	Δ_{AugLift}	Δ_{Depth}
1	ID	5.0%	6.7%
1	OOD	11.7%	9.2%
9	ID	4.3%	2.8%
9	OOD	7.6%	4.7%
27	ID	2.7%	1.9%
27	OOD	7.5%	5.8%
243	ID	1.4%	1.8%
243	OOD	8.3%	6.0%

AugLift provide a more generalizable signal than potentially brittle motion priors (discussed in Section 3.1), fortifying the model to OOD shifts. Furthermore, the final column (Δ_{Depth}) shows that adding only the depth cue to a model that already has confidence and temporal context continues to provide a large OOD boost (e.g., 6.0% at Seq-Len 243). This reinforces that the depth signal provides unique geometric information that is not captured by motion alone.

Qualitative Analysis. Figure 4 presents a qualitative comparison on challenging poses from the 3DHP test set. AugLift consistently produces more accurate 3D poses, especially in ambiguous scenarios like sitting and crouching where its additional depth and confidence cues are vital.

Inference Constraints. A key consideration is whether the generalization gains from AugLift justify its additional computational cost. We argue they do. The added latency is manageable, especially when compared to other components in the pipeline. For context, a common 2D detector like HRNet-W48 requires 44 ms for inference, and the MotionBERT lifter itself takes 16.7 ms. In contrast, using an

efficient depth model like Depth Anything v2 (small variant) adds only 13.3 ms of latency, a cost that is further amortized in streaming applications where depth maps can be computed periodically and reused across frames. While a more thorough analysis is warranted, this modest computational overhead is a worthwhile trade-off for the substantial OOD performance improvement. Additionally, developers can now choose to reduce sequence length in favor of AugLift’s rich spatial cues, achieving superior out-of-distribution performance within a given latency budget.

5 Conclusion

We introduced AugLift, a simple, modular input representation that enriches the standard 2D keypoint input for lifting-based 3D HPE with synergistic confidence and depth cues. Our extensive experiments show that this approach is a powerful mechanism for improving generalization without sacrificing in-domain accuracy. Across three training datasets and four distinct lifting architectures, AugLift consistently reduces out-of-distribution MPJPE by an average of 10.1% while also improving in-distribution performance by 4.0%. The gains are largest for short-sequence models, indicating that rich spatial cues can effectively offset temporal context. In addition, AugLift does not require a depth sensor or external data collection.

This work opens several avenues for future research. While our initial analysis shows that inferency latency is manageable, a more thorough study is warranted, and future work could explore distilling the depth model’s knowledge into a lightweight, unified architecture to enable real-time performance. Furthermore, our findings on the brittleness of motion priors suggest a need for deeper investigation into the role of temporal context; future research could explore how much the reliance on motion can be reduced when stronger per-frame inputs like AugLift’s are available. Finally, as this is the first work to demonstrate the power of this specific combination of cues, significant research remains in tuning AugLift’s hyperparameters and exploring other pre-trained priors to further unlock the potential of this approach.

References

- Chai, W.; Jiang, Z.; Hwang, J.-N.; and Wang, G. 2023. Global Adaptation Meets Local Generalization: Unsupervised Domain Adaptation for 3D Human Pose Estimation. In *Proceedings of the IEEE/CVF International Conference on Computer Vision (ICCV)*, 13404–13413.
- Chen, C.-H.; Tyagi, A.; Agrawal, A.; Drover, D.; Rohith, M.; Stojanov, S.; and Rehg, J. M. 2019. Unsupervised 3D pose estimation with geometric self-supervision. *Proceedings of the IEEE/CVF Conference on Computer Vision and Pattern Recognition (CVPR)*.
- Fieraru, M. M.; Zafir, M.; Pirlea, S. C.; Olaru, V.; and Sminchisescu, C. 2021. AIFit: Automatic 3D human-interpretable feedback models for fitness training. In *Proceedings of the IEEE/CVF Conference on Computer Vision and Pattern Recognition (CVPR)*.
- Gong, K.; Zhang, J.; and Feng, J. 2021. PoseAug: A differentiable pose augmentation framework for 3D human pose estimation. *arXiv preprint arXiv:2103.04265*.
- Ionescu, C.; Papava, D.; Olaru, V.; and Sminchisescu, C. 2014. Human3.6M: Large scale datasets and predictive methods for 3D human sensing in natural environments. *IEEE Transactions on Pattern Analysis and Machine Intelligence*.
- Jiang, L. 2021. Category Map Guided Ordinal Depth Prediction for 3D Human Pose Estimation. In *Proceedings of the IEEE/CVF Conference on Computer Vision and Pattern Recognition (CVPR)*. University of the Chinese Academy of Sciences, Institute of Automation: IEEE.
- Jiang, T.; Sun, Y.; Liu, Y.; Li, W.; Zhang, Z.; and Wu, W. 2023. Real-Time Multi-Person Pose Estimation based on MMPose. *arXiv preprint arXiv:2303.14384*.
- Li, Z.; Zhang, J.; Wu, Z.; Zhang, X.; Zhang, L.; and Luo, P. 2024. Depth Anything v2: Scaling up monocular depth estimation with large-scale pseudo-depth labels. *arXiv preprint arXiv:2401.07853*.
- Manzur, S.; Vela, B.; Vela, B.; Agrawal, A.; Dang-Vu, L.; Li, D.; and Hayes, W. 2025. PoseBench3D: A Cross-Dataset Analysis Framework for 3D Human Pose Estimation. *arXiv preprint arXiv:2505.10888*.
- Martinez, J.; Hossain, R.; Romero, J.; and Little, J. J. 2017. A simple yet effective baseline for 3d human pose estimation. In *Proceedings of the IEEE international conference on computer vision*, 2640–2649.
- Mehta, D.; Rhodin, H.; Casas, D.; Fua, P.; Sotnychenko, O.; Xu, W.; and Theobalt, C. 2016. Monocular 3D human pose estimation in the wild using improved CNN supervision. *arXiv preprint arXiv:1611.09813*.
- Nie, X.; Feng, J.; Zhang, J.; and Yan, S. 2019. Single-stage multi-person pose machines. In *Proceedings of the IEEE/CVF international conference on computer vision*, 6951–6960.
- Pavlakos, G.; Zhou, X.; and Daniilidis, K. 2018. Ordinal depth supervision for 3D human pose estimation. *arXiv preprint arXiv:1805.04095*.
- Pavlakos, G.; Zhou, X.; Derpanis, K. G.; and Daniilidis, K. 2016. Coarse-to-fine volumetric prediction for single-image 3D human pose. *arXiv preprint arXiv:1611.07828*.
- Pavlo, D.; Feichtenhofer, C.; Grangier, D.; and Auli, M. 2018. 3D human pose estimation in video with temporal convolutions and semi-supervised training. *arXiv preprint arXiv:1811.11742*.
- Rhodin, H.; Salzmann, M.; and Fua, P. 2018. Unsupervised geometry-aware representation for 3D human pose estimation. *arXiv preprint arXiv:1804.06254*.
- von Marcard, T.; Henschel, R.; Black, M. J.; Rosenhahn, B.; and Pons-Moll, G. 2018. Recovering accurate 3D human pose in the wild using IMUs and a moving camera. *arXiv preprint arXiv:1804.05184*.
- Wang, Z.; Shin, D.; and Fowlkes, C. 2020. Predicting camera viewpoint improves cross-dataset generalization for 3D human pose estimation. *arXiv preprint arXiv:2004.07980*.
- Xu, Y.; Wang, W.; Liu, T.; Liu, X.; Xie, J.; and Zhu, S.-C. 2022. Monocular 3D Pose Estimation via Pose Grammar and Data Augmentation. *IEEE Transactions on Pattern Analysis and Machine Intelligence*, 44(10): 6327–6344.
- Zheng, C.; Zhu, S.; Mendieta, M.; Yang, T.; Chen, C.; and Ding, Z. 2021. 3D Human Pose Estimation with Spatial and Temporal Transformers. In *Proceedings of the IEEE/CVF International Conference on Computer Vision (ICCV)*, 11656–11665.
- Zhou, F.; Yin, J.; and Li, P. 2024. Lifting by Image: Leveraging Image Cues for Accurate 3D Human Pose Estimation. In *Proceedings of the AAAI Conference on Artificial Intelligence*. Copyright © 2024, AAAI Press.
- Zhu, W.; Ma, X.; Liu, Z.; Liu, L.; Wu, W.; and Wang, Y. 2023. MotionBERT: A Unified Perspective on Learning Human Motion Representations. In *Proceedings of the IEEE/CVF International Conference on Computer Vision (ICCV)*.

Appendix A: Experimental Setup Details

This appendix provides additional details on our experimental setup, supplementing Section 4.1 of the main paper.

Prediction Tasks. The lifting literature considers two distinct settings: using ground-truth 2D keypoints (“GT setting”) and using detected 2D keypoints (“detection setting”). In the GT setting, 2D keypoints are obtained directly from dataset annotations, which eliminates noise and allows for controlled studies that isolate specific effects (e.g., the impact of sequence length). In the detection setting, keypoints are extracted from a 2D pose detector, which introduces real-world noise. Unless stated otherwise for a specific preliminary analysis, all main experiments in this paper are conducted in the detection setting to best align with practical applications.

Dataset Descriptions. Our experiments rely on four large-scale datasets. Human3.6M (H36M) (Ionescu et al. 2014) is a widely used indoor dataset featuring controlled motion sequences and fixed cameras; while densely annotated, its limited diversity can hinder generalization. In contrast, MPI-INF-3DHP (3DHP) (Mehta et al. 2016) introduces greater viewpoint diversity with more varied camera angles and occlusions. Fit3D (Fieraru et al. 2021) focuses on fitness-related motions with significant self-occlusions. Finally, 3D-Pose-in-the-Wild (3DPW) (von Marcard et al. 2018) was captured “in the wild” and includes complex activities like skateboarding, making it one of the most challenging benchmarks for real-world generalization.

Evaluation Details for 3DPW and Fit3D. To ensure fair comparisons, we made two dataset-specific adjustments. First, for 3DPW, we standardize the ground-truth skeletons to match the proportions of the H36M format by recentering the torso and proportionally adjusting the limbs. While performance is typically benchmarked on the official 3DPW test set, we evaluate on the full dataset, as it is used exclusively for OOD testing in our protocol and this provides a more comprehensive assessment. Second, for cross-dataset experiments requiring training on Fit3D, we create our own splits from the publicly available subjects (training on s03-s09, validating on s10-s11), as its official test set is held-out.

Implementation Note on PoseFormer. For the PoseFormer architecture, we report results using a sequence length of 27 frames. We successfully reproduced the 9-frame and 27-frame models from the original work to within a few millimeters of the reported MPJPE. However, despite extensive hyperparameter tuning, we were unable to replicate the results for the 81-frame model, a challenge that has been noted by other researchers in public forums.

Appendix B: AugLift Performance by Architecture

This section provides a high-level summary of AugLift’s performance across the four tested architectures, complementing the detailed results in the main text. The values in Table 6 are obtained by averaging the percentage improvements across the various input sequence lengths relevant to

Table 6: **Average performance gains from AugLift across different model architectures.** The table shows the percentage reduction in MPJPE, averaged over multiple sequence lengths for each backbone. Gains are shown relative to a standard baseline (Δ_{AugLift}) and a baseline that already includes 2D confidence scores (Δ_{Depth}).

Architecture	Split	Δ_{AugLift}	Δ_{Depth}
SimpleBaseline	ID	5.0%	6.7%
	OOD	11.7%	9.2%
PoseFormer	ID	1.1%	2.1%
	OOD	6.2%	5.6%
MotionBERT	ID	3.7%	1.6%
	OOD	10.2%	5.7%
VideoPose3D	ID	2.7%	2.6%
	OOD	5.9%	4.9%

Table 7: **Hyperparameter ablation for the SimpleBaseline + AugLift model, trained on H36M.** The top table shows the effect of varying dropout (with network depth fixed at 2 blocks), while the bottom shows the effect of changing network depth (with dropout fixed at 0.5). The batch size was 64 for all runs.

Dropout Ablation (blocks = 2)				
Dropout	H36M	3DHP	Fit3D	3DPW
0.25	54.6	97.1	72.2	163.2
0.33	54.7	96.6	72.5	163.6
0.42	54.9	96.0	73.9	164.4
0.50	56.0	96.2	77.2	167.8
Block-Depth Ablation (dropout = 0.5)				
Blocks	H36M	3DHP	Fit3D	3DPW
2	55.6	99.6	75.1	169.2
3	55.6	98.7	72.4	162.1
4	56.6	99.2	72.9	158.9

each model. Specifically, the sequence lengths averaged are: 1 frame for SimpleBaseline (Martinez et al. 2017); 9, 27, and 81 frames for PoseFormer (Zheng et al. 2021); and 9, 27, and 243 frames for both MotionBERT (Zhu et al. 2023) and VideoPose3D (Pavlo et al. 2018).

Appendix C: Additional Ablation Studies

To validate our design choices and explore training strategies, we performed several ablation studies. This included a hyperparameter search for the SimpleBaseline model and an investigation into the effect of our bounding box rescaling method at inference time. The results are presented in Table 7 (hyperparameter search) and Table 8 (bounding box rescaling analysis).

Summary of Findings. The results of our ablation studies show that the SimpleBaseline (Martinez et al. 2017) and VideoPose3D (Pavlo et al. 2018) models gain significantly

Table 8: **Ablation study on the impact of bounding box rescaling.** We report MPJPE (mm) on OOD datasets for models trained on H36M. "With Fix" refers to applying our rescaling method. The results show significant gains for SimpleBaseline and VideoPose3D on 3DPW, where the scale difference is largest.

Model	Dataset	No Rescaling	With Rescaling	Change
SimpleBaseline	3DPW	164.5	147.4	-10.0%
SimpleBaseline	3DHP	96.7	96.1	-0.6%
SimpleBaseline	Fit3D	75.1	75.2	+0.1%
VideoPose3D	3DPW	147.4	140.8	-4.5%
VideoPose3D	3DHP	89.9	89.8	-0.1%
VideoPose3D	Fit3D	75.0	75.5	+0.7%
PoseFormer	3DPW	126.7	131.8	+4.0%
PoseFormer	3DHP	84.1	86.1	+2.4%
PoseFormer	Fit3D	70.3	71.0	+1.0%

from the bounding box rescaling, particularly on the 3DPW dataset. PoseFormer (Zheng et al. 2021) shows negligible benefit from this component. As discussed in the main text, MotionBERT (Zhu et al. 2023) was omitted from this study as it already uses privileged focal-length and root-depth information in its camera-invariant codec, making our rescaling redundant.

Appendix D: Brittleness of Motion Cues

This section details our preliminary analysis on the generalization of temporal lifting models, which motivated the design of AugLift. To investigate the common assumption that longer motion sequences improve generalization, we performed a controlled study using the VideoPose3D (Pavlo et al. 2018) architecture. To isolate the pure effect of motion dynamics from detection noise, all models were trained on ground-truth 2D keypoints from H36M (Ionescu et al. 2014). To account for viewpoint changes, we also applied perspective camera augmentations during training (Gong, Zhang, and Feng 2021).

Our analysis reveals a surprising vulnerability of temporal models. As shown in Figure 5, while increasing the input sequence length consistently improves in-distribution performance on H36M, it fails to improve—and often degrades—cross-dataset performance on 3DHP, Fit3D, and 3DPW. This suggests models overfit to dataset-specific motion patterns. We tested this hypothesis by applying simple temporal transformations (e.g., reversing sequences or altering playback speeds) to create OOD motions from ID poses. Table 9 confirms that models using longer sequences are more sensitive to these transformations, underscoring their brittleness to motion variations not seen during training.

Appendix E: Deeper Dive into Spatial Cues

We investigated the potential of enriching the per-frame spatial input. We focused on ordinal depth (OD), which orders keypoints by relative depth (e.g., closer or farther from the camera) without estimating precise metric values. While

Table 9: **Overfitting to Motion Priors.** MPJPE on H36M validation using ground-truth 2D sequences. Simple temporal transformations (reversing, varying speed) significantly degrade performance for models using longer sequences, demonstrating overfitting to motion patterns.

Split	Seq 1	Seq 27	Seq 81	Seq 243
Train (Original)	25.1	16.6	15.7	13.4
Train (Reversed)	25.1	19.6	20.3	20.0
Train (Var. Speeds)	25.2	30.4	32.9	32.1
Val (Original)	39.8	39.3	38.6	37.1
Val (Reversed)	39.8	41.3	40.9	39.5
Val (Var. Speeds)	39.8	49.6	50.4	49.3

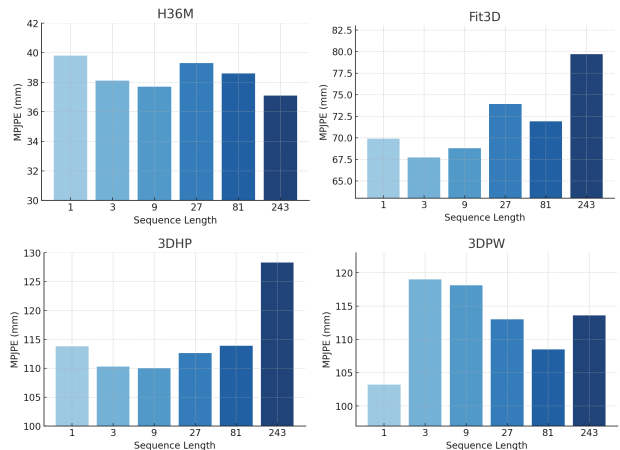


Figure 5: **Longer sequences can harm cross-dataset generalization.** While in-distribution error (H36M, top-left) decreases with sequence length, out-of-distribution error on other datasets stays flat or increases. This analysis used a VideoPose3D model in the GT setting.

prior work has used OD as a supervision signal (Pavlakos, Zhou, and Daniilidis 2018), its potential as a direct input to lifting models has been less explored. To quantify the maximum potential of this approach, we conducted an oracle study where we added a coarse OD signal to the 2D skeleton input. In this setup, keypoints are grouped into three categories—in front of, at, or behind the pelvis—using a fixed threshold on the ground-truth 3D data (e.g., 10cm). The compelling results of this study, which showed a significant reduction in generalization error, formed the primary motivation for AugLift.

E.1 Coarse Ordinal Depth experiments

Recall that this coarse ordinal depth (OD) signal is provided by an oracle, offering a lightweight spatial cue to complement the 2D keypoints. We tested the impact of this signal by discretizing each of the 17 joints into depth bins of varying coarseness, ranging from 1 cm to 25 cm. The results in Table 10 show that even at a coarse 25 cm granularity, the OD signal reduces generalization error on 3DHP by nearly 25%, despite requiring only 2.9 bins per frame on

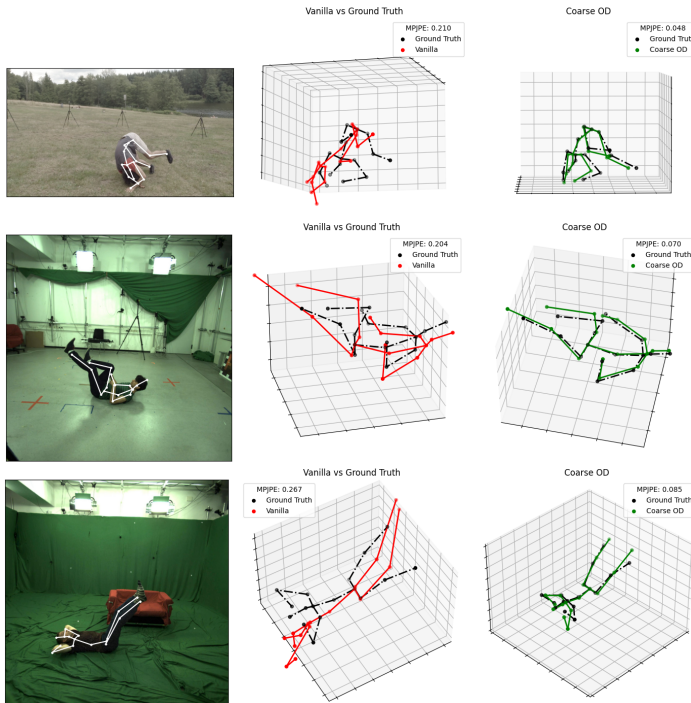


Figure 6: **Coarse ordinal depth (OD) greatly improves generalization by reducing depth ambiguity.** Each row compares the baseline lifting model (Vanilla) to the model augmented with oracle Coarse OD on 2D ground truth key-points.

average. This suggests that even a rough estimate of depth ordering—distinguishing which joints are in front of, in line with, or behind the pelvis—is highly informative for lifting models. Figure 6 provides a qualitative visualization of the significant improvements in the predicted 3D pose that result from leveraging these coarse OD cues.

E.2 Ablations on Coarseness of Signal

We study the impact of the amount of coarseness to the ordinal depth bins, to cross dataset performance in Table 10. While finer OD maps provide more depth detail, even a coarse three-bin OD (torso-depth, closer, farther) improves generalization, reducing MPJPE on 3DHP by 24.5% compared to standard lifting. This suggests that even lightweight ordinal depth cues provide strong spatial constraints, helping models better infer depth without overfitting to dataset-specific motion.

E.3 Comparison with Prior Work

In Table 11, we compare CoarseOD to perspective augmentations, and to Pavlakos 2018 (Pavlakos et al. 2016), demonstrating the effectiveness of adding depth cues and augmentation techniques in lifting-based 3D pose estimation. All models are trained on H36M and tested on 3DHP-INF, ensuring that performance is evaluated in a cross-dataset setting. The sequence length for TCN is set to 1 to isolate the

Table 10: **Coarser ordinal depth maps still improve generalization.** We analyze the impact of ordinal depth (OD) coarseness on cross-dataset performance.

Coarseness	GT Bins (H36M)	GT Bins (3DHP)	MPJPE (3DHP)
1 cm	13.7	13.8	52.6
10 cm	5.4	5.6	54.2
25 cm	2.9	2.9	61.2

Table 11: **Oracle CoarseOD significantly boosts cross-dataset performance.** CoarseOD improves generalization by 25% or more, showing that adding depth cues and perspective augmentation enhances cross-dataset performance. Models trained on H36M and tested on 3DHP-INF benefit from these cues, with CoarseOD + Perspective Aug achieving the highest accuracy.

Method	MPJPE ↓ (mm)	PMPJPE ↓ (mm)	3DPCK ↑ (150mm, %)	AUC ↑
Pavlakos 2018	—	—	71.9	35.3
Vanilla	94.4	63.1	81.4	48.8
Perspective Aug	81.1	57.4	86.8	53.9
CoarseOD	60.2	40.5	95.4	61.6
CoarseOD + Perspective Aug	53.1	36.9	97.2	65.5

impact of depth cues without reliance on temporal information. We report 3DPCK-150mm and AUC, as Pavlakos et al. do not provide MPJPE/P-MPJPE for the cross-dataset evaluation. Coarseness is set to 10cm, allowing for a balance between spatial granularity and robustness. The results show that CoarseOD + Perspective Aug achieves the best performance.